ROTOR BEARING LOADS WITH HONEYCOMB SEALS AND VOLUTE FORCES IN REINJECTION COMPRESSORS

by
Leonardo Baldassarre
Engineering Manager & Principal Engineer for Centrifugal Compressors
General Electric Oil & Gas Company
Florence, Italy
and
John W. Fulton
Senior Engineering Advisor
ExxonMobil Research and Engineering Company
Fairfax, Virginia

Leonardo Baldassarre is currently the Engineering Manager & Principal Engineer for Centrifugal Compressors with General Electric Oil & Gas Company, in Florence, Italy. He is responsible for all requisition, standardization, and CAD automation activities as well as for detailed design of new products for centrifugal compressors both in Florence (Nuovo Pignone) and Le Creusot (Thermodyn). Dr. Baldassarre began his career with General Electric Nuovo Pignone in 1997. He has worked as Design Engineer, R&D Team Leader for centrifugal compressors in Florence, Product Leader for centrifugal and axial compressors, and Requisition Manager for centrifugal compressors both for Florence and Le Creusot teams.

Dr. Baldassarre received a B.S. degree (Mechanical Engineering, 1993) and Ph.D. degree (Mechanical Engineering/Turbomachinery Fluid Dynamics, 1998) from the University of Florence. He has authored or coauthored 20 technical papers, mostly in the area of fluid dynamic design of 3D transonic impellers, rotating stall, and rotordynamics. He presently holds three patents.

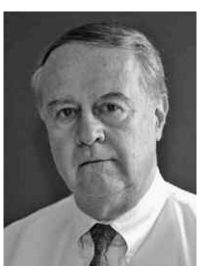

John W. Fulton is a Senior Engineering Advisor with Exxon Mobil Research and Engineering Company, in Fairfax, Virginia. In his 35 years with Exxon, he has worked in all phases of machinery engineering and in research and development. Mr. Fulton enjoyed years of assignments in Libya, Venezuela, Alaska, London, and Kuala Lumpur. He is co-inventor of six U.S. Patents.

Mr. Fulton has a B.S. degree (Mechanical Engineering) from New Jersey Institute of Technology.

ABSTRACT

The calculation for unbalance response of a rotor starts by calculating the bearing load to provide the basis for the bearing stiffness and damping characteristics. Measurements in test rigs at a major Texas university laboratory have shown that honeycomb-stator/drum-rotor annular seals can produce negative stiffness, in particular at zero to low whirl frequencies, which tends to pull the rotor off-center. Data given in this paper, from high-pressure factory tests of compressors using a honeycomb seal at the balance piston, have shown the rotor can be displaced from the usual position in the lower part of its journal bearing, degrading the unbalance response. In this paper the authors show that the honeycomb seal can produce a large disturbance in the equilibrium position of the rotor for certain values of negative stiffness, resulting in high bearing loads in unusual directions. It is also shown that aerodynamic forces on the rotor from the volute need to be considered.

INTRODUCTION

In the oil and gas industry, the typical centrifugal compressor for reinjection duty has its impellers placed in the casing between two bearings, with the shaft horizontal with respect to gravity. To calculate the vibration response of the rotor to unbalance, or the damped critical speeds (to evaluate rotordynamic instability) one has to know the bearing characteristics, which depend on the bearing loading. Most rotordynamic suites include a simple calculation that automatically finds the rotor weight and center of gravity. This calculation of static equilibrium then finds the load at each bearing by solving two equations, one found by setting the sum of forces equal to zero, and the other found by setting the sum of moments around one bearing equal to zero. This calculation will be shown in detail below.

This paper is motivated by experience with several compressors on full-load test. The specific compressors involved, and the operating conditions on test are given in Table 1.

Table 1. Specific Compressors and Operating Conditions.

Example	Casing Designation	Impeller Count	Speed	Rated Discharge bar (psi)
A	400	5	11250 RPM	237 (3440)
B	300	4	11250 RPM	407 (5900)
C	300	4	11000 RPM	760 (10600)

These compressors use a honeycomb seal running against a drum rotor for the balance piston. In contrast to labyrinth seals with teeth, or in contrast to rotors with labyrinth teeth running against honeycomb, the honeycomb/drum type seals have significant direct stiffness (defined more completely below). "Hole pattern" type seals running against drum rotors are similar. Because the test experience related in this paper was with honeycomb seals, not hole pattern type, this paper will discuss honeycomb seals only.

Figure 1 shows a photograph of the bore of a honeycomb seal. There are about 10,000 cells in this half of the seal. Each cell has a hexagonal width of about 2 mm (.08 inch) and a depth of about 2.3 mm (.09 inch). This seal is formed from a monolithic billet of aluminum, for all examples. In these examples the honeycomb seal acts on the balance piston that is just behind the last impeller.

Figure 1. Photo of a Honeycomb Seal.

These compressors also have a volute at the last impeller. The volute can produce asymmetric pressure gradients around the rotor. If the gas pressure is sufficiently high, then the asymmetric gradient may produce a radial force on the rotor that exceeds the rotor weight, as shown later.

EXPERIENCE ON FULL LOAD TEST

During full-load tests of compressor Example A, erratic response to unbalance was noted. Running at constant speed, the synchronous vibration varied from 6 to 25 microns peak-to-peak, as pressure and flow were varied. Clearly the high pressure gas was affecting the unbalance response of the rotor, either directly, or by affecting the bearing load, and thus the bearing dynamic characteristics. In an attempt to identify the cause, the pressure and flow were varied and repeated, over an appreciable range, as shown in Figure 2 and 3, respectively.

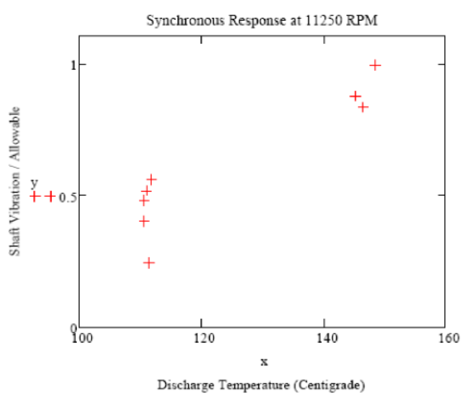

Figure 2. Synchronous Response (Filtered at 1 × RPM) of Compressor Example A at the Discharge End X-Probe as a Function of Discharge Temperature.

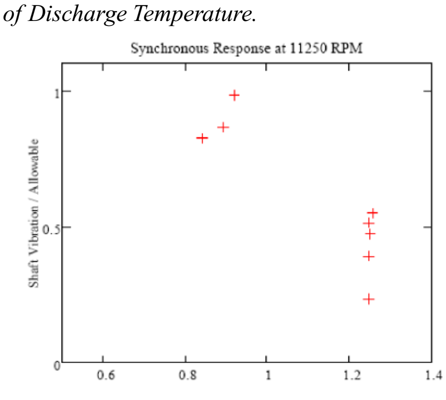

Figure 3. Synchronous Response (Filtered at 1 × RPM) of Compressor Example A at the Discharge End X-Probe as a Function of Suction Volume Flow.

From these figures it is clear that the change in unbalance response was well demonstrated, repeatable, and significantly affected. The three points at lower flow correspond to the three points at higher temperature. The separation of points is not as distinct when plotted against pressure.

From previous work by Camatti, et al. (2003), it is known that the forces produced by a honeycomb seal in high pressure gas are sensitive to the clearance of the leakage annulus. From finite element analysis of the honeycomb seal in this compressor, it is known that temperature changes the clearance and causes a taper in the clearance as well. Therefore it is not surprising that the rotor response could vary with discharge temperature, which sets the temperature of the seal, distorting the taper, and thus changing the honeycomb seal forces on the rotor. These changes apply to both the static force and the dynamic stiffness and damping coefficients acting synchronously.

It will be shown below, by calculation for the test stand conditions of Example C, that the volute force can exceed the rotor weight. The force and direction of the radial load produced by the volute depends on the ratio of volume flow to the design flow. Thus changing the flow can produce substantial additional load on the bearings, and thus affect their dynamic characteristics. Thus it is not surprising that the unbalance response might vary with volute-induced bearing loads. However, no practical method was obvious to distinguish between the bearing loads caused by the honeycomb seal versus the volute.

The rotordynamic stability of the Example A (and Example B, discussed below) compressors were excellent as tested. The response-to-unbalance was also within contract vibration limits. Therefore, an extensive investigation during full-load testing was not warranted, and an exact comparison of the rotor position on test and the position calculated below was not made. However, the effects on unbalance response in Example A were significant, and could have caused a problem, if the rotor response were not so well behaved in the base case. This gave motivation to find an analytic solution to understand the lifted rotor position that was observed and estimate the bearing loads that might occur.

In the case of Example B (and in other cases [Camatti, et al., 2003]) it was found that the proximity probes at the bearing journals showed the rotor journal was not resting in the bottom of the bearing when running, as assumed in the bearing load calculation that was outlined above. Instead the journal was often found in the top of the bearing, and the journal could be seen to lift as the compressor was started and loaded. Figure 4 shows the bearing journal position, measured by proximity probes, when the compressor was started and loaded. The left plot is for the balance piston end, and the right is the thrust end. The large circles represent the bearing clearance circle (nominal cold dimensions.) The parameter written by each point is revolutions per minute (rpm). The suction volume flow 76 percent of rated at full speed. From the calculated behavior of a tilt-pad bearing, one could expect that the journal should rise toward the center of the bearing, but not as high as the bearing center. Clearly, the journals in Example B rise above center, and more so, on the balance piston end.

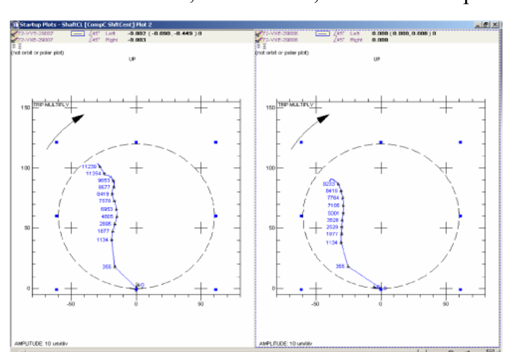

Figure 4. Bearing Centerline Position as Compressor Example B is Started and Loaded. The Plot on Left is the Balance Piston End and the Plot on Right is the Thrust End.

The tilt-pad bearings used on these compressors have thermocouples installed to measure the Babbitt temperature of the two bottom pads. On Example B, as a check on the validity of the journal center positions shown in Figure 4, one pad was moved from the bottom to the top of one bearing, with the second pad remaining in normal position. As expected from Figure 4, the top pad showed higher temperature than the bottom, confirming the load on the bearing was directed upward, and confirming the behavior shown there. The maximum temperatures measured were as shown in Table 2.

Table 2. Maximum Babbitt Temperatures.

Probe designation	location of pad	compressor end	Babbitt Temperature (Centigrade)
TE031A	top	DE (discharge)	86
TE031B	bottom	DE	69
TE030A	bottom	NDE (suction)	72
TE030B	bottom	NDE	71

Thus the top pad (72-TE-29031A) of the bearing near the balance piston is 17°C (62.6°F) hotter than the bottom pad, indicating a substantially larger load on the top pad. Just to give a complete picture, these temperature records are plotted versus time in Figure 5.

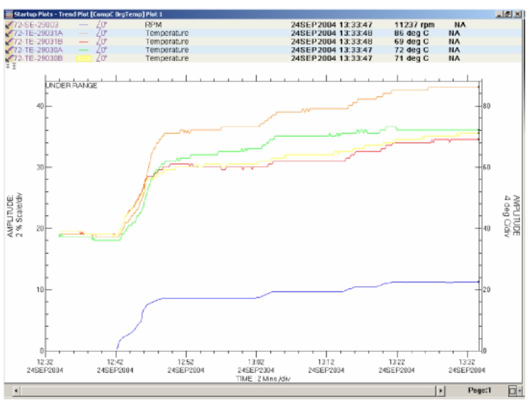

Figure 5. Trend Plot of the Bearing Pad Temperatures (Top Four Traces) on Example B, Bottom Trace is Speed in RPM.

CALCULATING THE EFFECT OF HONEYCOMB SEAL ON STATIC EQUILIBRIUM OF THE ROTOR

Because both the potential honeycomb seal force and the potential volute force could be responsible for the anomalous journal position and bearing loads discussed above, the two effects were investigated by calculations after the testing was complete. The bearings themselves were not suspected of causing the anomalous position, as multiple disassemblies to change dry gas seals during some of the testing did not implicate them. On one instance with Example B, an increase once-per-revolution vibration prompted a bearing inspection that showed faulty assembly. However correcting this did not eliminate the anomalous position. The remainder of this paper will discuss the results of the calculation.

As a basis for understanding the calculations, it is necessary to compare and contrast the general behavior of the honeycomb seal direct stiffness and the volute force as follows:

- The balance drum/honeycomb seal was next to the volute (as usual) in the above cases, so that it was not obvious by comparing the behavior of the bearing on one end of the casing to the other, whether the honeycomb seal or the volute was responsible for the anomalous journal position in the bearing, as might be expected from the static equilibrium calculations.
- The honeycomb seal forces are effectively proportional to the displacement of the drum within the honeycomb seal running clearance, That is, they have the characteristic of a spring rate that can be measured in Newtons per meter (pounds per inch).
- The volute forces change as the flow rate changes with respect to the design (best efficiency) flow. Of course their magnitude changes with pressure. However, the volute forces are independent of small changes of the rotor position within its running clearance. That is, the volute force does not have the characteristic of spring.
- The honeycomb seal spring rates are extremely sensitive variation of the running clearance along the length of the drum. A well-considered finite element analysis of the drum and of the honeycomb seal is necessary to define the clearance along the length as a function of temperature, pressure, shaft speed, and mounting conditions. Changes in these variables during testing may change the static equilibrium of the rotor position.
- The honeycomb seal spring rates in both the direct and cross-coupled directions are strong functions of the whirl frequency of the drum orbital motion. For calculation of static equilibrium the displacement occurs at zero whirl frequency.
- Honeycomb seal spring rate, K, in the direction of drum displacement may affect the first bending frequency of the rotor. This reduced whirl frequency can fall into the range where the honeycomb has negative damping. This can cause rotordynamic instability, resulting in catastrophic vibration. Such a problem is reported in a previous paper (Camati, et al., 2003) but is not of concern here as the subject compressors were very stable.

The honeycomb seal spring rates were calculated using the seal code developed by Kleynhans and Childs (1997). The volute forces were calculated using a computational fluid dynamics code. Figure 6 shows the coordinate system used. In a free body diagram for static equilibrium all forces are considered to be acting *on* the rotor. Lhc is the distance from Bearing 1 to the center of the honeycomb seal.

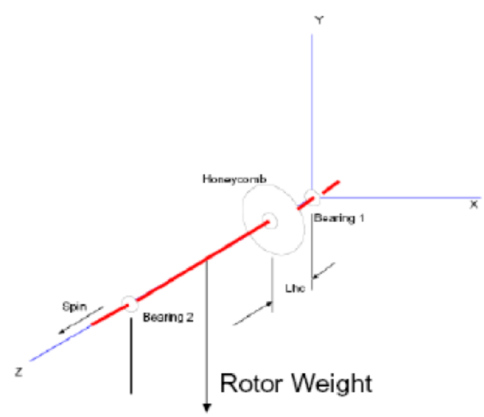

Figure 6. Rotor Coordinate System.

The simple calculation of the bearing load in the typical rotordynamic code uses two equations. The sum of the forces, and the sum of the moments, must be equal to zero, for static equilibrium. For the simple calculation without the honeycomb seal, it is not necessary to know the spring rates of the bearings as one can find the two bearing loads with the two equations. The static equilibrium can be written by summing the forces to zero (Equation 1) plus summing the moments to zero (Equation 2). Only the vertical plane need be considered, as there are no horizontal forces.

$$fb1 + fb2 - Wr = 0 \qquad \textbf{(1)}$$

$$Lcg \cdot Wr - Lcl \cdot fb2 = 0 \qquad \textbf{(2)}$$

The standard model for forces acting on the rotor is given in Equation (3) (Kleynhans and Childs, 1997).

$$\begin{pmatrix} Fx \\ Fy \end{pmatrix} = -1 \cdot \left[\begin{pmatrix} K & k \\ -k & K \end{pmatrix} \cdot \begin{pmatrix} X \\ Y \end{pmatrix} + \begin{pmatrix} C & c \\ -c & C \end{pmatrix} \cdot \begin{pmatrix} Xdot \\ Ydot \end{pmatrix} \right] \quad \textbf{(3)}$$

For static equilibrium, the velocities Xdot and Ydot are zero, which eliminates the damping coefficients, C and c, from consideration. This equation can be applied to the static force caused by the honeycomb seal acting on a rotor, as expressed by Equations (4) and (5):

$$Fh_y(x, y) := kh \cdot x - Kh \cdot y \quad \textbf{(4)}$$

$$Fh_x(x, y) := -Kh \cdot x - kh \cdot y \quad \textbf{(5)}$$

In Equations (4) and (5) the direct stiffness is K and the cross-coupled stiffness is k. Note that the cross-coupled stiffness requires that the horizontal displacement be included in the equations for vertical forces and vice versa. The subscript y indicates the force from the honeycomb acts in the y (vertical) direction and the subscript x indicates action in the horizontal direction.

When the honeycomb seal is added, there are now three unknown force vectors, the two force vectors of the bearings on the rotor and now the force vector of the honeycomb seal on the rotor. However, there are only two force equations (one in the horizontal direction and one vertical) and two moment equations. Thus the calculation becomes a "statically indeterminate" problem (Popov, 1968), because the force caused by the honeycomb seal depends on its drum displacement.

Six equations are required to solve for the six displacements. Two force balances are provided by Equations (6) and (7) and two moment balances are provided by Equations (8) and (9).

$$\frac{Fb_y(x1, y1) + Fb_y(x2, y2) + Fh_y(x3, y3) - Wr}{Wr} = 0 \quad \textbf{(6)}$$

$$\frac{Fb_x(x1, y1) + Fb_x(x2, y2) + Fh_x(x3, y3)}{Wr} = 0 \quad \textbf{(7)}$$

$$\frac{Lcg \cdot Wr - Lhc \cdot Fh_y(x3, y3) - Lcl \cdot Fb_y(x2, y2)}{Wr \cdot Lcl} = 0 \quad \textbf{(8)}$$

$$\frac{Lhc \cdot Fh_x(x3, y3) + Lcl \cdot Fb_x(x2, y2)}{Wr \cdot Lcl} = 0 \quad \textbf{(9)}$$

To account for the cross coupling, the forces are written as functions of both horizontal (x) and vertical (y) displacements. The force balance equation is normalized by rotor weight, Wr, to suit the tolerance limit of the numerical method used. The moment equations are normalized by moment Wr × Lcl.

Figure 7 shows the displacements in the vertical direction as defined by Equation (10).

$$\frac{y1 + \frac{Lhc}{Lcl} \cdot (y2 - y1) + \frac{Fh_y(x3, y3)}{Krotor} + yhc_{static} - y3}{HCradclear} = 0 \quad \textbf{(10)}$$

That equation gives the displacement of the rotor drum at the honeycomb seal, y3. The first term, y1, is the displacement of the bearing at the coordinate origin. The second term uses the displacement of the second bearing, y2, to find the centerline displacement at the honeycomb seal location. The third term represents the bending of the rotor due to gravity. The fourth term gives the displacement due to rotor bending under force from the honeycomb seal. The displacements in the horizontal plane, shown in Equation 11, are similar but of course do not include bending due to gravity.

$$\frac{x1 + \frac{Lhc}{Lcl} \cdot (x2 - x1) + \frac{Fh_x(x3, y3)}{Krotor} - x3}{HCradclear} = 0 \quad \textbf{(11)}$$

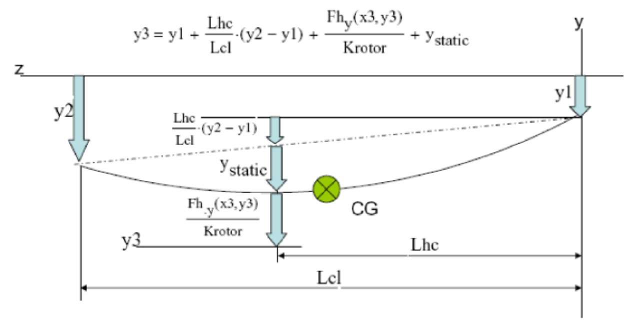

Figure 7. Definition of the Rotor Displacements in the Vertical Plane.

The spring coefficient representing the rotor bending stiffness is easily found by using a rotor response code to calculate an asynchronous response at very low frequency (1 Hertz) to find the displacement at the honeycomb seal caused by an asynchronous force at the honeycomb location

As mentioned, Equation (10) also includes the displacement of the rotor at the honeycomb seal location, yhc_{static} due to rotor weight. It is handled separately as it remains constant while the other displacements in Figure 6 vary. Handling it separately avoids complication due to the weight action not being at the honeycomb seal location. For the examples given, yhc_{static} is a significant term. The authors estimated it from the first bending frequency of the rotor, using the concept of the resting displacement of a single spring-mass oscillator. The yhc_{static} is adjusted for the actual bending curve of the rotor, using the concept of the Raleigh natural frequency method, using the first bending mode shape as calculated by a rotordynamic code.

This system can be solved for the six particular values of displacement, using a standard numerical solution method. Because the force equations are written as functions of displacement, no further algebra is required when using the solver in a popular technical calculation software. Figure 8 shows the result graphically in the same format as used in Figure 4. Please note that the direction of rotation as viewed in Figure 4 is clockwise, while it is counterclockwise as viewed in Figure 8. (This reverses the horizontal displacements between the two figures, as the view is from opposite ends of the rotor.) The displacements are normalized by their respective clearance circles to indicate the limit of validity of the solutions, due to contact if a displacement exceeds the clearances. The honeycomb seal clearance is larger than the bearing clearance. The displacement of the seal drum is marked by the solid triangle symbol, bearing 1 (near the honeycomb seal) by the circle, and bearing 2 by the square.

When the honeycomb seal bore is not concentric with the centerline between the two bearing bores, a variable called "offset" can be introduced to represent the honeycomb bore position. To include this in the above calculation, the offset must be included in the right-hand side of Equations (4) and (5) by adding it to the variable displacements.

The honeycomb seal stiffness and damping, calculated by the seal code developed by Kleynhans and Childs (1997) are −0.150 E9 N/m (−0.857 E6 lbf/in) and 0.200 E9 N/m (1.142 E6 lbf/in), respectively. These values are for a honeycomb seal with diverging clearance. They are for the compressor of Example B, but with slightly different internal parts, and slightly lower pressure and speed than tested for Figure 4. The cross-coupled stiffness causes the rotor center to be displaced to one side, instead of remaining under the center of the tilt-pad bearing (which has no cross-coupled stiffness).

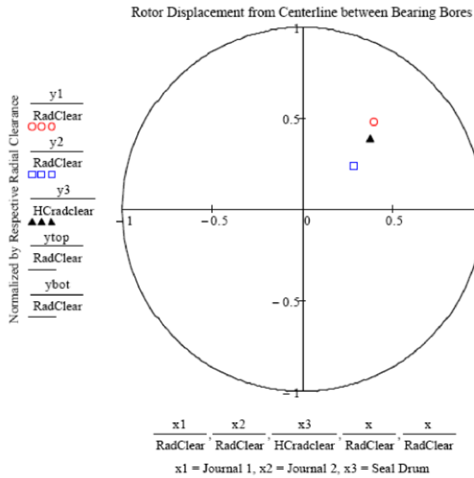

Figure 8. Journal and Drum Positions in their Clearance Circles—Example B. Alternate Bundle, Diverging Clearance in Honeycomb, 9965 RPM.

Figure 8 represents only one value of honeycomb seal direct and cross-coupled stiffness. The behavior of the static equilibrium calculation varies dramatically with direct stiffness of the honeycomb seal, when negative direct stiffness is considered. Figure 9 shows this vertical displacement of the honeycomb seal drum as a function of honeycomb direct stiffness, over a range of negative seal stiffness, with all other input values held constant. In this figure, the drum displacement is normalized by its radial clearance while the honeycomb seal direct stiffness is normalized by the bending stiffness of the rotor calculated at the seal location. The expected value of the direct stiffness is marked by the line labeled "expected." At the expected stiffness, the rotor is displaced upward to the level marked by the line labeled "Root2," thus explaining how the bearings may run against their top pads as shown in Figure 4.

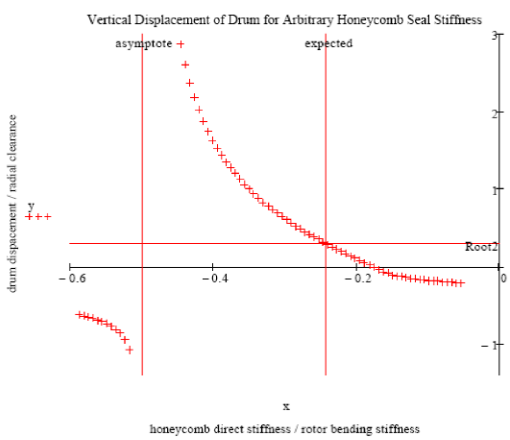

Figure 9. Vertical Force on Bearing Journals as a Function of Arbitrary Direct Stiffness of the Honeycomb Seal.

As the honeycomb seal stiffness becomes more negative, the upward displacement increases at a larger rate, reaching 100 percent of its clearance. If it were not limited by rubbing, the calculated displacement would increase without bound, to reach the line labeled "asymptote." Going further left to more negative values and the displacement suddenly changes direction downward to negative values. This system of equations indicates very large forces on the bearings near a particular value of honeycomb seal stiffness. Mathematically, the force is unbounded and approaches an asymptote (defined in Thomas, 1968) located at a particular magnitude of direct stiffness of the honeycomb.

A GRAPHICAL ILLUSTRATION OF THE ASYMPTOTIC BEHAVIOR

The following explanation is intended to aid visualization of how the asymptotic behavior occurs. It is based on the concept of solving two simultaneous equations graphically. To show the concept of the graphical solution, consider two simultaneous Equations (12) and (13) (where a, b, c, and d are numerical constants):

$$y = a * x + b \quad \textbf{(12)}$$

$$y = c * x + d \quad \textbf{(13)}$$

Each equation can be plotted as a straight line on x-y coordinates. If the two equations are independent and consistent equations that apply simultaneously, then their solution (a particular value of x and of y that satisfies the equations) is found where the two lines cross (Ayres, 1958).

To form the first line of the graphical solution, conduct a "thought experiment" on the rotor. Take the rotor running on its bearings. Apply an arbitrary force in the positive vertical direction *on* the rotor at the location were the honeycomb seal acts. Measure the displacement of the rotor at that location. Plot the arbitrary force on the Y axis and the resulting displacement on the X axis. This is done in Figure 10, forming the red line, Y1. The slope of the red line represents the stiffness of the rotor-bearing system. This slope is not constant here because the static bearing stiffness acts only in the direct axis and is not cross-coupled for the tilt-pad bearings used. The nonlinearity is included in the analysis to accurately portray the bearing characteristic at high eccentricity. Figure 11 shows the values used.

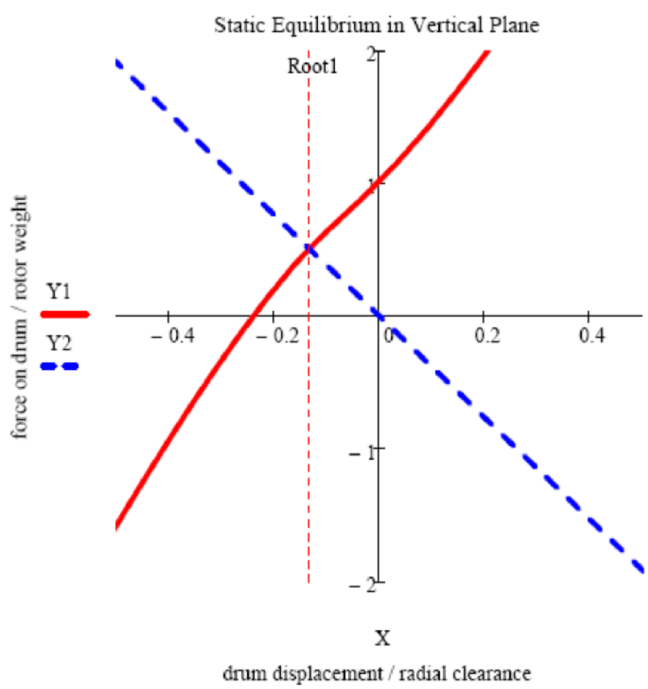

Figure 10. Graphical Solution with Positive Honeycomb Seal Stiffness.

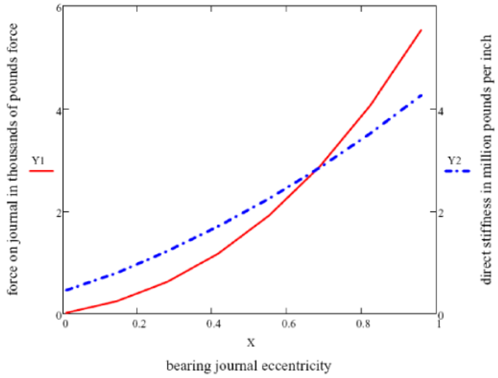

Figure 11. Bearing Force and Bearing Static Stiffness, as a Function of Eccentricity.

If the force at the honeycomb seal position is zero, the equilibrium position occurs where the red line crosses the X axis (force is zero there). In this instance, one can see in Figure 10 that equilibrium occurs at about 25 percent of the radial clearance below the center of the honeycomb seal. (The X axis of the plot represents the honeycomb seal drum vertical displacement normalized by radial clearance of the seal. The Y axis is force on drum normalized by rotor weight, Wr.)

Now do another experiment. Center the rotor drum in the honeycomb seal and lift the rotor up. For a honeycomb seal with positive stiffness the honeycomb seal will resist with a downward (negative) force *on* the rotor. Do this for a series of points and plot as the blue line (Y2) as done in Figure 10. The stiffness of the honeycomb seal in this plot is minus one times the slope of the blue line.

The two lines represent two equations that are solved where the lines cross. The static equilibrium occurs where the red and blue line cross, which is about 15 percent of the radial clearance above the center of the honeycomb seal, at the vertical line marked "Root1." This is expected, as the positive stiffness of this honeycomb seal is helping to support the rotor, lifting it up from the 25 percent position (below center) found without considering the honeycomb seal support. Knowing the force and displacement at the seal, the moment balance equation can be used to solve for the force at bearing two, and then the force balance equation can be used to solve for the force at bearing one.

To demonstrate how the bearing load reaches the asymptote when the negative stiffness of the honeycomb increases, the above plot will be repeated with a honeycomb seal stiffness that has a slope near the slope of the rotor characteristic (red). This represents a honeycomb seal having negative stiffness. That is, as the drum is displaced away from the center, the honeycomb seal tends to pull the drum further off center. Figure 12 shows this graphical solution for rotor equilibrium in the vertical plane with *negative* honeycomb direct stiffness.

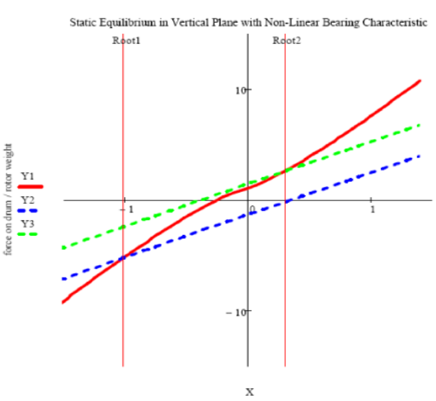

Figure 12. Graphical Solution for Rotor Static Equilibrium for Negative Stiffness of the Honeycomb Seal.

The graphical solution is also useful to show honeycomb seal offset from the bearing centerline. In Figures 10 and 12 the blue line is offset from the center representing an upward displacement of the honeycomb bore. The green line is offset by an equal and opposite amount showing a low honeycomb bore. The possible range of solutions for this offset falls between the blue and green lines, representing an acute sensitivity to concentricity.

In Figure 12 the red and blue lines cross near 100 percent of the radial clearance below the honeycomb sea, at the displacement marked "Root 1." This intersection is the equilibrium position. Note that with negative stiffness small changes in the slope of the blue line can move the crossing point with the red line to very large positive or negative values, thus representing large forces on the bearings. Of course, checking this graphical solution against the algebraic solution, shown earlier, gives identical results. However, the graphical solution gives more insight.

From this graph, the learning is to avoid negative stiffness whose absolute value is near the stiffness of the rotor bearing system, that is, near the asymptote. Note that the position of the asymptote depends on the stiffness of the rotor bearing system as well as the stiffness of the honeycomb seal. Even larger negative stiffness, to the left of the asymptote may create a larger problem, as it is likely to depress the whirl frequency (typically the first bending mode) possibly causing the honeycomb to produce negative damping, and thus causing rotordynamic instability.

Actually plotting the graph is not necessary to find the solution, as the intersection of the rotor and honeycomb seal characteristic lines is easily found by setting the equations for the two lines equal and finding the displacement of the rotor in the honeycomb seal that satisfies the two equations. However plotting the graph is useful to visualize if the solution is near the asymptote.

For a rigid rotor solution it is possible to solve for the asymptote in closed form based on the lengths of the components along the rotor. Given two identical bearings of stiffness Kyy, the critical honeycomb negative stiffness where the asymptote occurs is shown in Equation (14).

$$Kcrit := (-Kyy)\cdot\frac{Lb^2}{Lb^2 + 2\cdot Lhc^2 - 2\cdot Lhc\cdot Lb} \quad \mathbf{(14)}$$

This equation only applies for zero offset.

BEHAVIOR DISPLAYED BY THE GRAPHICAL SOLUTION

For practical application, rotor bending, rotor sag due to gravity, honeycomb seal offset from the bearing centerline, and bearing nonlinearity are usually highly significant. The honeycomb seal offset needs to be controlled by tolerances, or by adjustment on assembly.

For the compressor of Example B, all these effects were included in the calculation of static equilibrium. Figure 12 gives the graphical solution for this case. The red line shows the force-displacement characteristic of the rotor-bearing system. It shows a hardening spring rate due to the tilt-pad bearing reaching high eccentricity, as found by a Reynolds code for laminar flow in bearings.

In Figure 12, the dashed green line shows a honeycomb seal with negative stiffness, whose center is displaced 60 microns (2.3 mils) *below* the bearing centerline, shown on the graph as a displacement to the left on the horizontal axis, at about 40 percent of the radial clearance of the honeycomb seal. The intersection of the red and green lines shows the equilibrium position in honeycomb seal just above center (Root2). The dashed blue line shows a honeycomb seal with negative stiffness, whose center is displaced 60 microns (2.3 mils) *above* the bearing centerline, shown as a displacement to the right on the horizontal axis. The intersection of the red and blue lines shows the calculated equilibrium position of the drum in the honeycomb seal would heavily depress the rotor below its centerline. The displacement normalized by the honeycomb seal's radial clearance is near minus one, indicating the drum is close to rubbing the honeycomb surface at the calculated equilibrium.

This behavior may be self-limiting, because if the rotor drum rubs the honeycomb seal surface, then, given a rotor whirl amplitude approaching the honeycomb seal clearance, the surface will be worn to give an axial leakage path of constant clearance. Based on calculations using the seal code developed by Kleynhans and Childs (1997), such a clearance does not usually have significant negative direct stiffness.

Note that the red line is nearly parallel with the blue and green ones, which are offset by the concentricity tolerance on the position of the honeycomb seal. *The practical result is that the static equilibrium cannot be accurately calculated in this case*, because the intersections within the tolerance band cover a range from where the drum is near the bottom of the honeycomb to being lifted above the centerline of the two bearings.

The behavior of the rotor when it is near the asymptote can be understood by the concept of "indifferent equilibrium." This concept applies to the case were all spring rates in the system are linear. Indifferent equilibrium is most easily seen by an example where the honeycomb seal (with negative direct stiffness) is at the center span of a symmetric rigid-rotor bearing assembly.

In that case the asymptote will occur when the honeycomb stiffness is equal to minus the sum of the bearing stiffness (twice the stiffness of the two identical bearings.). *Thus the rotor will have zero stiffness to parallel translation, because the negative honeycomb seal stiffness will cancel the positive bearing stiffness, as the three spring rates are additive because the springs act in parallel*. (The resistance to angular displacement will remain.)

At this asymptote, if the rotor moves a honeycomb seal with negative stiffness will pull it up, and the bearings will push down, giving a zero net force resisting the displacement. Therefore this rotor can be moved to any lateral position without applying an external force, assuming perfectly linear stiffness. (Nonlinear stiffness of the bearing or honeycomb seal may not cancel at all displacements.) When the solution for static equilibrium is at the asymptote, a rotor is indifferent to its lateral position, and can be moved to different positions with little or no force, provided the rotor drum does not hit the honeycomb bore. However, the forces on the bearings can be very large.

INFLUENCE OF VOLUTE FORCES ON ROTOR STATIC EQUILIBRIUM

In contrast to the honeycomb seal, which is characterized as a spring rate, the volute forces can be represented as a static force on the rotor, independent of small displacements of the rotor. They can then be incorporated into the above static equilibrium model in the same manner as the weight of the rotor. As a simplification, the volute force can be applied at nearly the same location as the honeycomb seal force. However, obtaining a good estimate of the volute force is laborious.

In order to calculate the force generated by the volute a complete computational fluid dynamics (CFD) model of the last impeller plus diffuser plus discharge volute has been developed. The analysis has been carried out using the well-known mixing plane approach. According to this technique the complete model has been divided in two parts: first the impeller plus the first part of the diffuser, second the diffuser plus the discharge volute. First analysis is done on the impeller by imposing the boundary conditions at the inlet plus the mass flow. Once this calculation is completed total pressure and total temperature distributions as well as yaw angle are extracted at the interface plane and are used as boundary conditions for the CFD analysis of the volute. This analysis also requires imposing the mass flow (the same value applied for the CFD analysis of the impeller).

The analysis is able to capture the static pressure gradients in the tangential directions close to the outlet of the impeller. By knowing the pressure distribution at the outlet of the impeller as well as the geometry of the impellers, diaphragm-impeller cavities and seals it is possible to calculate the resulting radial force by means of a static equilibrium analysis. Figure 13 shows a cross section of last wheel stage of a reinjection compressor, Example C.

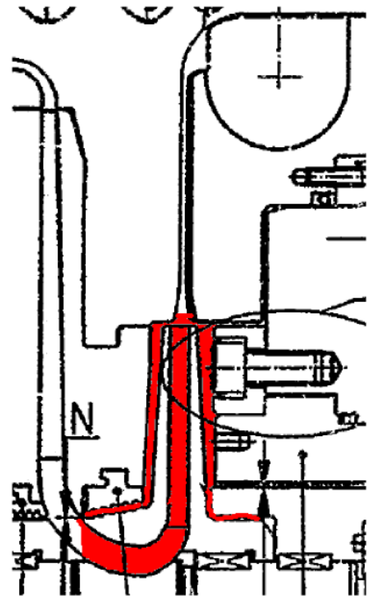

Figure 13. Cross Section of Last Wheel of a Tested Compressor.

The control volume used to make the static equilibrium of the impeller is highlighted in red color. For the analysis the authors assumed that the pressure gradient extends down to the diameter of inlet eye seal on the impeller cover, and down to the hub at the foot of the impeller disk. Pressure gradients have been considered constant along the two cavities. This assumption leads to make an overestimation of the forces.

Figure 14 shows the result of the above analysis applied to a very high pressure compressor, Example, C for the full density full pressure conditions in the authors' testing facility. In particular circumferential pressure gradients are evident.

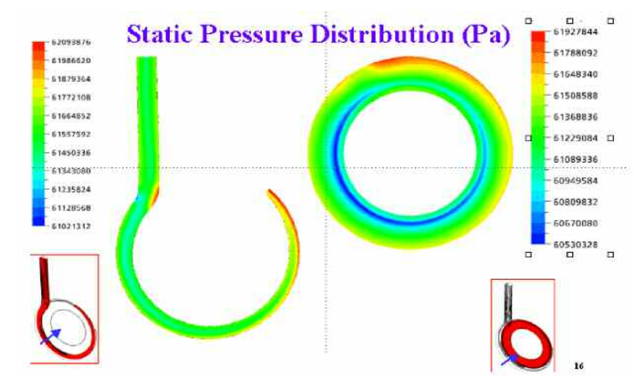

Figure 14. Static Pressure Distribution Around the Last Impeller.

Figure 15 is a graph showing the static pressure distribution immediately at the discharge of the impeller and used in order to compute the radial force created on the rotor. For this case the pressure equilibrium of the rotor control volume leads to a horizontal force of −9561 N (−2149 lbf) and vertical force of 9663 N (2172 lbf). The sum of these forces acts at an angle of 45 degrees from vertical, as shown in Figure 16. The weight of the rotor is 350 kg (771.62 lb), i.e., the vertical force from the volute is around three times the weight. The negative value means that the force is in the same direction of the weight.

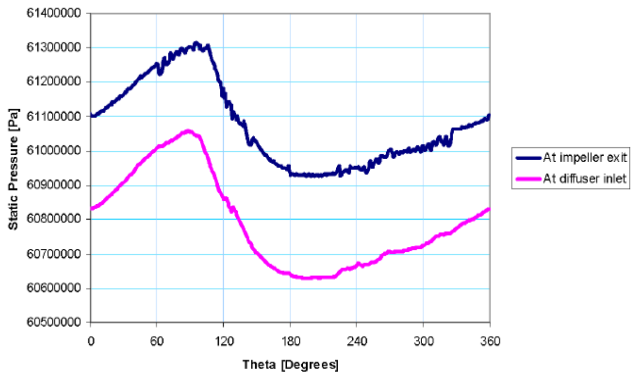

Figure 15. Pressure Profile around Circumference of Last Impeller.

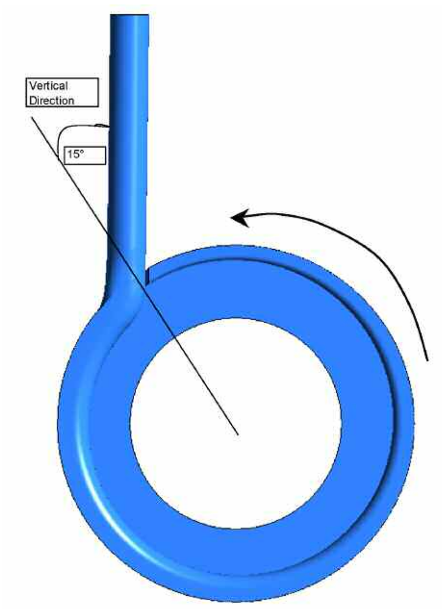

Figure 16. Direction of Net Force Due to Pressure.

Although this particular example is not correlated to the test data, is serves to demonstrate that the volute forces can dominate rotor weight for compressors in this size and pressure range.

COMPARISON OF CALCULATIONS WITH TEST DATA

The honeycomb seal stiffness values used in this paper were all calculated with the seal code developed by Kleynhans and Childs (1997). For Examples A and B, using a diverging clearance (leakage area increasing going downstream) in this seal code gives negative direct stiffness. A converging clearance gives positive direct stiffness of the honeycomb seal.

The honeycomb seal for Example B was modified after the measurements in Figures 4 and 5 were made. The modification was made when an opportunity arose to limit the possibility of high bearing loads. Swirl brakes were used on the honeycomb seal to avoid subsynchronous instability. Using the operating (hot and spinning) clearance of the honeycomb seal for Example B, the calculated direct stiffness at zero frequency before and after changing the clearance is shown in Table 3 for the respective clearances.

Table 3. Calculated Direct Stiffness at Zero Frequency Before and After Changing the Clearance.

	Radial Clearance at Honeycomb Inlet	Radial Clearance at Honeycomb Outlet	Keff (0 Hz)
	mm (mils)	mm (mils)	N/m (million lbf/in)
Initial tests	0.15 (5.9)	0.18 (7.1)	-0.58e8 (-0.33)
As modified	0.25 (9.8)	0.18 (7.1)	+0.25e9 (+1.43)

After the honeycomb seal was modified to have positive stiffness the compressor was retested. The measured bearing journal positions are shown in Figure 17. The journal in the nondrive-end (NDE) bearing did not lift high but is pushed to the side. The journal in the drive-end (DE) bearing (next to the honeycomb seal) still lifted to the top pads. The volute forces were not calculated, as the effort was not justified by the good behavior of the compressor.

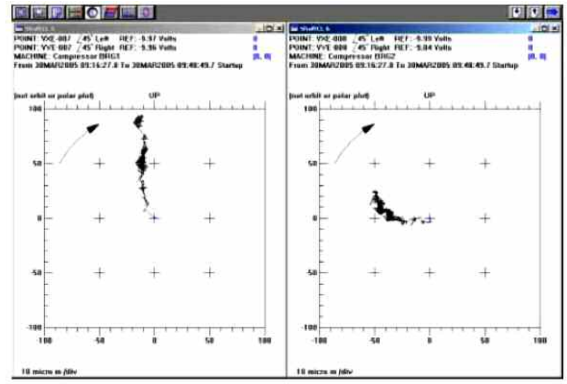

Figure 17. Calculated Static Force by Bearings for Example B, before Modification of the Honeycomb Bore.

Figure 18 shows the calculated static force on the rotor by bearings for Example B before modification of the honeycomb bore. The operating conditions for Figure 18 are estimated to correspond to Figure 4 at maximum speed. The offset used corresponds to the green line in Figure 12. The vertical line labeled "expected" in Figure 18 represents the Keff shown in the above table for the rated conditions. At the expected Keff, the forces at both bearings are negative, pushing down on the rotor, in the same direction as shown in Figures 4 and 5. Note that the bearing force is large, being nearly twice the rotor weight on bearing number one. Because the volute forces are not considered, the calculation is not empirically confirmed. However, the calculated and measured journal conditions are not contradicted either.

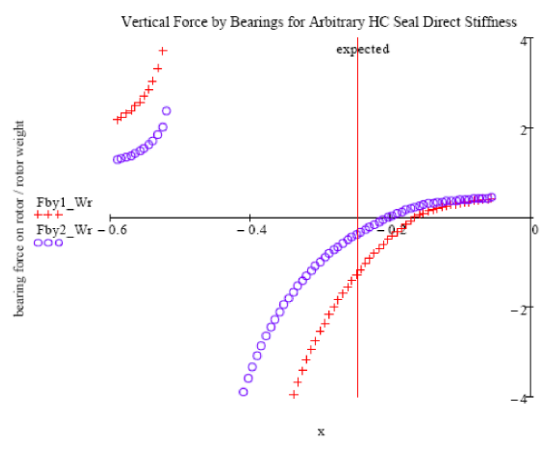

Figure 18. Journal Positions in the Bearings of Example B after Revising the Honeycomb Seal.

Figure 19 shows the calculated force on the rotor by the bearings for Example B as modified. The offset used corresponds to the blue line in Figure 20.The vertical line labeled "expected" represents another value of the Keff = +0.259 E9 N/m (+1.43 E6 lbf/in) for the as-modified conditions. At the expected Keff, the force from Bearing 1 (on the DE of the rotor) is pushing down, as shown on the right-hand side of Figure 19. At the expected Keff, the force from Bearing 2 (on the NDE of the rotor) is pushing down slightly, as shown in the right-hand side of Figure 19. Note that the Bearing 2 force is small, with its absolute value being less than half the rotor weight. Without the honeycomb seal force or volute forces, the bearing force would be about half the rotor weight, pushing up. The graphical solution predicting the rotor equilibrium as modified is shown in Figure 20.

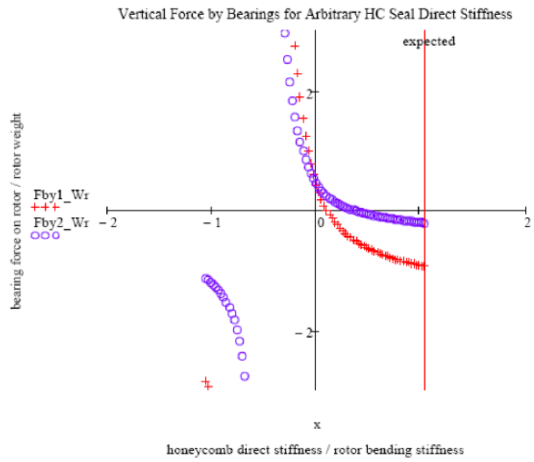

Figure 19. Calculated Static Force by Bearings for Example B, after Modification of the Honeycomb Bore.

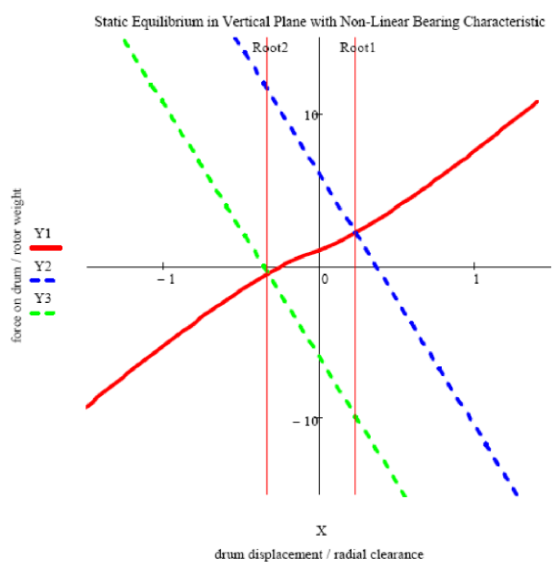

Figure 20. Graphical Solution Corresponding to Figure 19.

Figures 19 and 20 are consistent between the calculation and test, assuming a known offset (tolerance) of the honeycomb bore. However, the actual offset is not known. Note that the offsets are opposite between Figures 19 and 18. The actual offsets were unknown. Alternate compressor internal parts (rotor and bundle) were installed for the test shown in Figure 17 than were used in the test shown in Figure 4. Therefore, the offsets may have changed between Figure 18 and 19.

DISCUSSION

The basic assertion of this paper is that honeycomb seal and volute forces in reinjection compressors can invalidate the bearing load calculations typically used in rotordynamics analysis to find the bearing characteristic. A practical solution is to use high preload and tight clearances on tilt-pad bearings to make the bearing less sensitive to load. The disadvantage of high preload and tight clearances is loss of opportunity to maximize the bearing damping and thus optimize unbalance response and rotordynamic instability.

The measured rotor position in the bearings of the examples was often against the top pads, in opposition to the standard assumption of gravity load. A more unexpected conclusion, from the equations of static equilibrium, is that a honeycomb seal having a negative static stiffness in the same range as the rotor-bearing system stiffness (that is, at the asymptote) can produce bearing loads of many times the rotor weight. These calculations suggest that such a load would only be bounded by contact of the rotor against the honeycomb (based on a linear stiffness characterization of the honeycomb). However, the contact force will be small due to the indifferent equilibrium effect discussed above. (The large force on the rotor in the honeycomb is carried by the gas pressure.) In the cases presented, the calculations predict the asymptote was not reached. Only moderate contact was noted on disassembly.

The solution of the six equations of equilibrium (Equations 6 through 11) is straightforward and well based on the theory of statically indeterminate problems (Popov, 1968.) However, conceptually graphic solution gives more insight into the behavior of the system.

The concept of static equilibrium could also be applied to honeycomb seal test rigs used for determining the dynamic coefficients. In the case of test rigs where the seal carrier moves with respect to a stiffly supported rotor, the direct stiffness of the tie-rod assembly could be used in the calculation in place of the rotorbearing system stiffness. When testing seals with negative direct stiffness contact with the rotor may occur. The graphical solution presented in this paper shows such contact will occur when the absolute value of negative stiffness of the honeycomb approaches the positive stiffness of the mechanical parts of the system (when approaching the asymptote). This is conceptually different from reaching contact only at very large values of negative stiffness.

The test results presented prove that the bearing loads are not due to gravity alone, as it is customary to assume. The calculations presented here confirm that negative stiffness from the honeycomb seal, and volute loads should have a dramatic effect on the static equilibrium of the rotor on its bearings. Due to strong influence of the unknown magnitude and direction of offset between the honeycomb bore and the bearing centerline, the calculations suggest the bearing loads are not calculable, given typical offset tolerances. Furthermore, the aerodynamic force on the rotor can vary so that the estimated bearing loads may vary over a wide range. "Indifferent equilibrium" further confounds the problem.

Nevertheless, the analysis presented requires that the compressor design must take the variability of the possible bearing loads into consideration. For oil film bearings this is easily considered in the design stage by calculating the loads at the extremes of offset. Magnetic bearings and bearings supported on squeeze film dampers typically have direct stiffness that is an order of magnitude softer than the tilt-pad journal bearings used in Examples A and B. If magnetic bearings or damper bearings are used with a honeycomb seal, especially one having negative stiffness, the calculated asymptote would occur at a much smaller negative stiffness of the honeycomb seal than with stiffer bearings. Such behavior could disrupt the functioning of a magnetic bearing or damper bearing even if the honeycomb negative stiffness were relatively small in absolute value.

CONCLUSIONS

Calculation of the bearing load based on only the rotor weight (for horizontal rotors) is not valid for high pressure centrifugal compressors having honeycomb/drum-rotor seals, or single-volute or collector type discharge hardware. The forces caused by these components are shown for the above examples to exceed the rotor weight.

Introducing the honeycomb/drum type seal into the bearing load calculation as direct and cross-coupled spring coefficients makes the problem statically indeterminate and thus requires consideration of displacement of the journal in its bearing, the drum in the honeycomb bore, and the rotor as a beam in bending. In this case the bearing loads can be solved by the standard methods of the mechanics of solids.

When the spring coefficient of the honeycomb seal is negative, the indeterminate beam calculation can show asymptotic behavior. In this case the drum displacement will only be limited by contact with the honeycomb seal bore. At the asymptote, the rotor can be either lifted or depressed.

This paper introduces a conceptually graphical solution to the indeterminate beam calculation for the purpose of visualizing the asymptotic behavior (here shown in a vertical plane.) This solution also makes clear the importance of small deviations of the honeycomb bore from the centerline between the two bearings.

The asymptotic behavior does not depend merely on the magnitude of the negative stiffness of the honeycomb seal, but instead depends on the ratio of that stiffness to the stiffness of the rotor bearing system. In the graphical solution this occurs when the slope of the honeycomb seal displacement versus force line is nearly parallel with the slope of the rotor-bearing system displacement versus force line.

This solution predicts the rotor can be lifted in its bearings by the negative stiffness of the honeycomb seal, at sufficiently high gas pressures. This solution also predicts that the rotor can be lifted in its bearings by positive stiffness of the honeycomb seal, when the honeycomb bore is offset above the centerline between the two bearings.

For examples given in this paper, these predictions are not inconsistent with the observed behavior. However, the unknown values of honeycomb bore concentricity defeat an exact calculation, because the bearing position is acutely sensitive to the honeycomb bore offset. The volute forces compound this problem.

NOMENCLATURE

fb1	N (lbf)	= Vertical load on bearing number 1
fb2	N (lbf)	= Vertical load on bearing number 2
Wr	N (lbf)	= Vertical force due to rotor weight
Lcg	mm (inch)	= Horizontal distance from bearing 1 to the rotor center of gravity
Lhc	mm (inch)	= Horizontal distance from bearing 1 to the rotor center of the seal
Lcl	mm (inch)	= Distance between horizontal centers of the two bearings
$Fb_x(x1,y1)$	N (lbf)	= Force by the bearing on the rotor in the horizontal direction due to displacements x1 (direct) and y1 (cross-coupled)
$Fb_y(x1,y1)$	N (lbf)	= Force by the bearing on the rotor in the vertical direction due to displacements y1 (direct) and x1 (cross-coupled)
$Fh_x(x3,y3)$	N (lbf)	= Force by the honeycomb seal on the rotor in the horizontal direction due to displacements x3 (direct) and y3 (cross-coupled)
$Fh_y(x3,y3)$	N (lbf)	= Force by the honeycomb seal on the rotor in the vertical direction due to displacements y3 (direct) and x3 (cross-coupled)
K N/m	(lbf/in)	= Radial spring coefficient of linearized restoring direct force
k	N/m (lbf/in)	= Tangential spring coefficient of linearized cross-coupled force
C	N*s/m (lbf*s/in)	= Damping coefficient—direct
c	N*s/m (lbf*s/in)	= Damping coefficient cross-coupled
x1, x2	microns (mil)	= Horizontal displacement of rotor in bearing 1 and 2, respectively
y1, y2	microns (mil)	= Vertical displacement of rotor in bearing 1 and 2, respectively
Xdot	mm/sec (in/s)	= Horizontal velocity of whirl orbit
Ydot	mm/sec (in/s)	= Vertical velocity of whirl orbit
Kyy = K	N/m (lbf/in)	= Bearing direct stiffness in the vertical direction
Lb	mm (inch)	= Lcl
Kcrit	N/m (lbf/in)	= Honeycomb seal stiffness at asymptote for the rigid rotor, linear bearing case
Keff	N/m (lbf/in)	= Direct stiffness of the honeycomb seal at zero frequency

Subscripts

1	= Bearing 1
2	= Bearing 2
3	= Drum of honeycomb seal

REFERENCES

Ayres, F. Jr., 1958, *First Year College Mathematics,* New York, New York: McGraw-Hill Book Company, p. 28.

Camatti, M., Vannini, G, Fulton, J., and Hopenwasser, F, 2003, "Instability of a High Pressure Compressor Equipped with Honeycomb Seals," *Proceedings of the Thirty-Second Turbomachinery Symposium,* Turbomachinery Laboratory, Texas A&M University, College Station, Texas, pp. 39-48.

Kleynhans, G. W. and Childs, D. W., 1997, "The Acoustic Influence of Cell Depth on Rotordynamic Characteristics of Smooth-Rotor/Honeycomb-Stator Annular Gas Seals," *Journal of Engineering for Gas Turbines and Power, 119,* pp. 949-957.

Popov, E. P., 1968, *Introduction to Mechanics of Solids,* Englewood Cliffs, New Jersey: Prentice-Hall, Inc., Chapter 12, "Statically Indeterminate Problems."

Thomas, G. B., Jr., 1968, *Calculus and Analytic Geometry,* Fourth Edition, Reading, Massachusetts: Addison-Wesley Publishing Company, p. 317.

BIBLIOGRAPHY

Mathcad, 2007, Version 14, Parametric Technology Corporation, Needham, Massachusetts.

Wagner, N. G., 1999, "Reliable Rotor Dynamic Design of High Pressure Compressor Based on Test Rig Data," Transactions of the ASME, Journal of Engineering for Gas Turbines and Power, October 2001, *123,* pp. 849-856.

ACKNOWLEDGEMENTS

The authors thank General Electric Oil & Gas, and ExxonMobil Research & Engineering for permission to publish this paper. Many thanks also to Luca Poli for his support and contributions, and also to Vittorio Michelassi in particular for the contribution given in the aero CFD analysis.